International Journal of Railway Technology
Volume 1, Issue 2, Pages 89-113, 2012.
doi:10.4203/ijrt.1.2.5

SAXE-COBURG
PUBLICATIONS

The Qualitative Influence of Model Parameters on the Dynamic Response of a Viaduct

A.H. Jesus, Z. Dimitrovová and M.A.G. Silva
UNIC, Department of Civil Engineering
Nova University
Portugal

Abstract

The qualitative influence of several model parameters on the dynamic response of a railways viaduct, modelled after an actual structure located in Santana do Cartaxo, Portugal, is analysed through a parametric statistical analysis. Two-level factorial experimentation was carried out with the help of a parametric model of the viaduct developed with ANSYS APDL. The range of values admitted for the key parameters and the corresponding deviations from mean values were evaluated from data made accessible by the road authorities and experience. For the sake of simplicity only one axle load was applied on a single module of the viaduct. It was concluded that the analysis of individual effects is satisfactory to obtain key results based on maximum displacements. Nevertheless, regarding peak accelerations, especially at the viaduct deck, interaction effects are important and the influence of key parameters cannot be analysed individually. Therefore, simultaneous consideration of several key parameters provides a better representation of reality associated with the application of statistical analysis.

Keywords: dynamic analysis, railway bridges, key input data, key results, factorial experimentation, design of experiments.

1 Introduction

The dynamic analyses of railway bridges is still a subject of research given the uncertainties of both material characterization and the numerical procedures associated with the model selected to represent the system. One problem derives from the fact that criteria to establish the response quantities required to define the dynamic response of bridges are not universally accepted and that fact prevents the set up of general rules and strategies for adequate numerical procedures. Although simplified models of railway tracks are widely used, complete models involving all structural details are preferable when structural nonlinearities are important to the response quantities of interest to the designer.

Over the years, various types of bridge models have been used in studies on bridge dynamics and, therefore, an extensive general review would be unnecessarily lengthy. Initially, continuum models of simply-supported Euler–Bernoulli beams were by far the most popular, because of their simplicity and ability to lead to closed-form solutions ([1-3]). Recently, Euler–Bernoulli beams were utilized in a study on a bridge–track–train interaction in [4]. However, practical applicability of the continuum models is limited to bridges of simple configuration.

On the research of the dynamics of bridges under moving loads, three main types of models are used: (i) the moving force model; (ii) the moving mass model; and (iii) the moving system model that comprehends a system of masses, springs and dampers. The moving force model, that considers only gravitational effects of the load and completely neglects its inertia and the interaction with the bridge, is a very simple, yet realistic representation of the moving load in the cases where the mass of the load is small in comparison with the mass of the bridge. The moving mass model considers gravitational as well as inertia effects of the load but neglects the elastic and damping properties of the suspension and vibrations of the sprung masses of the vehicle. Similar to the moving force model, it cannot realistically predict the response of the vehicle. The moving system model considers effects neglected in the previous two load models and can vary from a single-degree of freedom system [5], also referred to as the sprung mass, through a two-degree of freedom system [3], to a more complex multi-degree of freedom system, capable of very realistic simulation of the vibrations of railway vehicles [6]. This model is necessary when studying passengers' comfort and vehicle stability. It is not necessary for the analysis presented in this paper. In addition, unevenness of the rail was also omitted [7] despite being a significant factor in the dynamic response of the rail-track, and especially of the vehicle, because it would require treatment beyond the scope of this paper.

According to [8] a moving force model can be safely used if the ratio of the load mass over the mass of the bridge does not exceed 30%. The ratio of the mid-span deflection by the amplitude of the force is shown to be very similar for a moving force and moving suspension over a full range of velocities until the critical one, even if the aforementioned ratio reaches 50% [5]. This conclusion is also supported in [9].

Theoretically, the problem of the moving load was first tackled for the case in which the mass of the beam was considered small against the mass of a single constant load. The original approximate solution is attributed to R. Willis [10]. G.G. Stokes [11] and H. Zimmermann [12] approach the problem under similar assumptions. The other extreme case, *i.e.* that of the load mass being small against the mass of the beam, was originally examined for a simply supported beam and constant concentrated force by A.N. Krylov [13] using the method of expansion into eigenfuncions, and by S. P. Timoshenko [14], A.N. Lowan [15] and N.G. Bondar [16] who solved it with the aid of Green´s functions and integral equations, respectively.

Advances in computational technology and numerical methods allowed for accurate and efficient modelling of complex structures using the finite element method. Extensive reviews of several techniques can be found in monograph [9].

Design engineers often rely completely on the output originated from finite element (FE) calculations and seldom have the opportunity to check the accuracy of the results obtained. Railway bridges, in turn, are complex structures that require simplifications and always imply uncertainties present in their dynamic analysis. Statistical methods analyses have the potential to mitigate some of those limitations despite being often overlooked and seldom used by structural engineers. Factorial experimentation applied to the dynamics of bridges is quite scarce but can be found in [17] and related works of the first author of this recent article.

Performing statistical analyses satisfies at least three classes of objectives.

First of all, by statistical analysis of numerical results obtained it is possible to establish a set of key input data and key results. In this context, key input data are defined as those whose change causes the largest changes in key results. Traditionally, at each stage, only the influence of one input parameter was analysed, but, recently, the importance of studying the joint effect of several modelling parameters has been proven.

Secondly, a very important aspect to consider when a numerical model of a complex structure like a railway bridge or a viaduct is developed for running dynamic analyses is the posterior calibration of input data by experimental verification. In-situ measurements are quite expensive and what to measure and where to do it must be carefully studied. When statistical analysis is made, then the key results determined identify the characteristics to be measured by in-situ experiments. The key input data serve for model calibration, and at the same time dictate additional tests to be performed in a laboratory environment, in order to provide better estimates of the values to be used in the numerical model.

Finally, by considering the variations of key parameters in accordance with the uncertainty of the actual values, it is possible to establish a range of actual responses and probability of their occurrences.

Most previous work on parametric analyses of railway bridges considered the influence of key parameters individually, leading sometimes to contradictory conclusions. One can, for instance, compare the conclusions in [5] and [6]. It is seen that dynamic amplification factor of mid-span displacement with respect to the velocity for the ratio of the load mass over bridge mass equal to 50% varies between these two works even for lower velocities. For higher velocities the results presented in [6] reverse the expected influence, meaning that lower mass ratios induce a higher dynamic amplification factor, which differs from the conclusions made in [5, 9] and those also reported in [8]. Moreover, in analyses presented in [5, 6], all model parameters are fixed and a selected response quantity at one point of the bridge is analyzed against velocity. Simultaneous consideration of the influence of several key parameters provides a better representation of reality associated with the application of statistical analysis.

The work presented in the sequel was performed as part of a project named SMARTRACK dedicated to research in the area of the integrated response of trains, railways and supporting structures. One of the case studies selected by the industrial partner of the project, REFER EP, was a segment of track including a viaduct located in Portugal, in Santana do Cartaxo, and a database from REFER was used for definition of the relevant data. After some preliminary work, selected key input

data were (A) ballast stiffness; (B) concrete stiffness; (C) soil stiffness; (D)train speed; (E) ballast damping; and (F) rail pad damping. Except for the train velocity, their variation was established according to characteristics of the project and considered as uncertainties in data specification. For the train speed, a variation of 3% was considered, a value felt realistic according to the database of circulation vehicles provided by REFER. All variables are therefore treated as qualitative.

Two levels of full and fractional analyses have been analysed, [18]. It is necessary to point out, that the resulting data are the output of FE analysis and, therefore, there is no error associated with experimentation, because the FE results on the same model are unique. Given the summary above, it is now possible to define the objectives of this paper:

(i) To establish which FE results can be analysed by individual effect;
(ii) To establish which FE results should be analysed by interaction effect;
(iii) To establish dominating factors for results from (i);
(iv) To establish guidelines for future work, that will analyse final response probability.

Statistical analyses require several runs in a model that parametrically varies the input data and automatically extracts necessary output. Therefore numerical models must be computationally accessible and provide results with sufficient accuracy.

The numerical model is developed in an ANSYS/LS-DYNA module. The parametric analyses with automatic extraction of key results are coded by APDL (ANSYS parametric design language) [19].

Several simplifying structural assumptions were introduced: (i) rail-pads and ballast are represented by springs and dampers; (ii) rails, sleepers, pillars, foundation blocks and piles are approached by beam elements; (iii) shell elements are used for the viaduct deck; (iv) only a part of soil layers is modelled by three-dimensional elements.

The reflection of waves at the model boundaries is prevented by damping elements defined by Lysmer´s absorbing boundary condition [20], and soil layer above the rock foundation is substituted by representative springs [21]. Lateral springs simulate the effect of the surrounding soil.

The mass per unit of length of the viaduct (*e.g.* of the concrete deck with the superstructure is 23.4ton/m) is significant when compared to the distributed mass of the train (*e.g.* the locomotive CP5600 is 4.2ton/m) and for this reason the load mass is neglected. Such analysis cannot predict the response of the vehicle; thus, it cannot be used in the applications where the direct assessment of passengers' comfort is of interest, but this aspect is beyond the objectives of this paper.

This paper is based on previous work by Jesus *et al.* [22], introducing substantial changes in the finite element model, detailed analysis of the results obtained, factors variation in accordance with data uncertainty, and a comparison of the conclusions of full and fractional analyses. The main contribution of this work lies in the application of factorial analysis to a fairly detailed model of a viaduct. It is worthwhile to underline that in several comparison analyses like the ones from [5] and [6], the bridge is modelled by a simply supported beam. The model of a bridge in [17] is more detailed, but it is composed mostly by beam elements. In the model presented in this paper, several structural details are included, like rail-pads, ballast,

foundation soils, and the deck is represented by shell elements. The model is created from fully parametric input, and it therefore allows for an easy introduction of material non-linearities and changes in geometrical arrangements.

The paper is organized in the following way: in Section 2 the case study is described; in Section 3 the FE model and its variants are defined, and in Section 4 the results of statistical analyses are shown, compared and discussed. Conclusions appear in Section 5.

2 Case study

Necessary information regarding the structure, train specification and *in-situ* measurements of the properties of the soil foundations was supplied by REFER EP [23]. The case study corresponds to a location in the Portugal North Line, second sub-link Setil Sul Vale de Santarém, which develops from km 56+625 until km 65+287 and is part of the rehabilitation of the North Line. The Santana do Cartaxo segment, where a new railway is included over a viaduct built at km 59+000 to km 60+000 (Figure 1), is an exception in the rehabilitation which otherwise closely follows the original design.

The viaduct is composed of a set of eight module sections in the longitudinal direction. Each module is connected to the other through transition pillars which are larger and have more piles than the intermediate pillars. The spans linked to the transition pillars were enlarged by 3m to make up for expansion joints of 6m. Each module always has the same type of intermediate pillars to support the deck. There are 46 pillars with a height around 4.2m, resting on concrete blocks, each connected to two piles. The piles have a diameter of 1.5m and can reach a depth of 30 to 35m.

Figure 1: Santana do Cartaxo viaduct: general view (left); embankment (right)

One of the eight modules comprises three spans of 25, 30, and 25m, totalling a length of 80m, while the other seven modules have spans of 25, 4x30 and 25m, yielding the total length of 170m, bringing the total viaduct length to 1312m.

On the plan view (see Figure 2) the viaduct develops linearly and, at the end a left transition curve of the final radius 1750m starts.

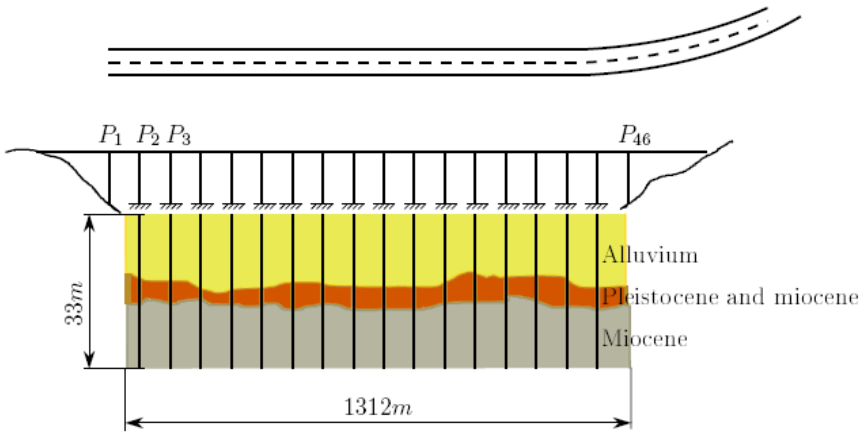

Figure 2: Viaduct plan and longitudinal view showing the soil geological composition

According to the geological prospecting data, the stratigraphy classification (Figure 2) revealed the presence of:

- Alluvium (14m)
- Pleistocene and Miocene (5m)
- Miocene

This last substratum can be characterized as an effectively stiff soil.

Geotechnical unit	μ [kN/m^3]	G [MPa]			v	E [MPa]	
		γ=10^{-6} (G_0)	γ=10^{-4}	γ=10^{-3}		γ=10^{-4}	γ=10^{-3}
Clay and sits ("A1")	16	19.8	19.8	10.9	0.49	59	32.5
Fine sand and siltose clays ("A2" and "A3")	18	36	28.8	14.4	0.35	77.7	38.9
Over-consolidated clays ("P-M")	20	66.1	59.5	36.4	0.48	176.1	107.7
Miocene ("M")	21.5	350	298	157	0.25	745	392.5

Table 1: The relevant geological data

The relevant geological data for each substratum (soil constants) are given in Table 1, where μ, E, G and v stand for volumetric weight, Young´s modulus, shear modulus and Poisson´s ratio, respectively. γ represents shear deformation. The values presented were obtained experimentally by *in-situ* tests and are reported in [23]. The alluvium layer is classified into three groups, designated A1, A2 and A3. P-M and M stand for the Pleistocene and Miocene and Miocene, respectively.

A typical viaduct deck cross-section is shown in Figure 3 and the superstructure geometry in Figure 4.

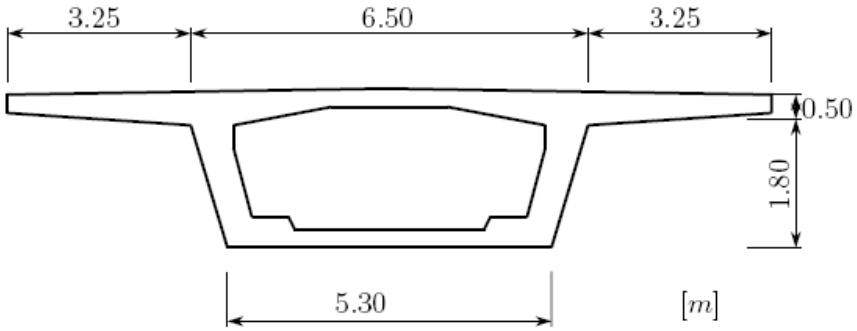

Figure 3: Viaduct deck cross-section

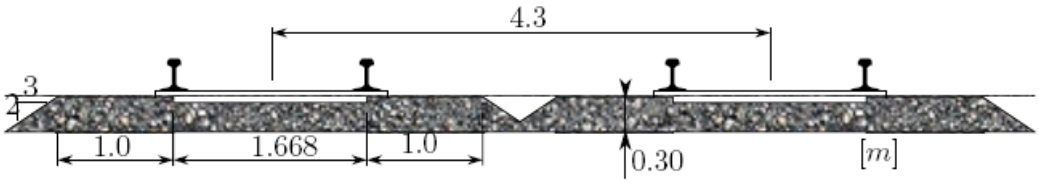

Figure 4: Superstructure geometry

The traffic over the viaduct is practically equally distributed between Alfa Pendular and Intercidades trains (Figure 5), travelling at a maximum speed of 220km/h. There are also passages by the regional train, but this one traverses the viaduct at a lower speed, with a maximum value established as 190km/h.

Figure 5: Alfa Pendular train (left); Intercidades train (right)

3 Finite element model

3.1 General considerations

The application of the finite element method (FEM) to computationally model the system requires careful choices of (i) types of elements; (ii) size of model; (iii) size of the finite elements; and (iv) treatment of boundary conditions. As specified in the introduction, the model was coded parametrically in APDL and only the first of eight modules, the one having three spans of 25, 30 and 25m, is modelled as a straight line. This module assents at its ends on two embankments, 30m long each, which are represented by springs and dampers. Through this article, the longitudinal axis is denoted as "z", the axis that is normal to the lateral faces of the soil is taken as "x", and the vertical axis is "y".

In order to run statistical and parametric analyses, the finite element model must be computationally accessible. This is the reason why an explicit solver was chosen and thus an APDL code of the three-dimensional FE model was created for the explicit dynamic module LS-DYNA of ANSYS. Nevertheless, an APDL code had also to be developed for the implicit module in order to evaluate natural frequencies and shapes. Separate developments were necessary, because element types are different for explicit and implicit modules. Material behaviour was assumed linear in both cases.

Several structural simplifications that keep the computational effort at a tractable level were introduced. Rail-pads and ballast are represented by linear and rotational spring and damper elements acting in three directions, in the same way as reported in [24]. Rails, sleepers, pillars, foundation block and piles are approached by beam elements. The viaduct piers are modelled with a rectangular section and are connected at the top to the shell elements that represent the lower deck. The connection allows for rotation in the longitudinal direction, *i.e.* around x-axis. The viaduct piles and foundation block are idealized as a pair of beams connected by a third concrete block. Beam elements are superposed directly on the edges of soil elements to avoid additional constraints. Shell elements are used for the viaduct deck. Only a part of the soil layers is modelled by three-dimensional elements. The surrounding soil is modelled by representative springs and dampers. Springs should represent the rigidity of the surrounding layers and dampers should ensure smooth wave propagation into surrounding layers without reflections from the artificial boundary [25].

The applied load corresponds to one axle load of Intercidades locomotive. The value of 213kN was rounded to 200kN, giving a force equal to 100kN applied at each rail. Reference velocity was selected as 180km/h=50m/s.

The critical velocity v_{cr} of a load moving on a simply supported beam is derived *e.g.* in Frýba [3] as:

$$v_{cr} = 2 f_{(1)} L \tag{1}$$

where $f_{(1)}$ is the fundamental frequency and L is the beam length. By using the

numerical value of 4.73Hz, which corresponds to the first bending mode and essentially excites the middle span of 30m length (see Table 2), the critical velocity yields 284m/s. Therefore the critical velocity of the load is not of concern.

Resonance resulting from the successive passage of equidistant loads or groups of loads, as it is described *e.g.* in monograph [9], is briefly examined. The resonance velocity $v_{n,j}^{res}$ is derived as:

$$v_{n,j}^{res} = \frac{f_{(n)} d}{j} \tag{2}$$

where d is the distance between the loads, $f_{(n)}$ is n-th natural frequency in Hz and j is an integer. The distance of bogies in the Intercidades locomotive CP5600 is 10.5m. This means that by using 4.73Hz, which corresponds to the first bending mode, the first resonance velocity is below the reference velocity. The distance between the bogies of the carriages is 18m, thus the corresponding resonance velocity is higher than the reference velocity, but it does not form multiples of the reference velocity. By changing the train type, the distances between the bogies are altered and, therefore, the influence of consecutive loads is also different. Variations in reference velocity thus may induce effects related to resonance and a sudden change in the structural response. For this reason, the velocity variation was small and the effect of consecutive loads was not examined. This effect will be included in further studies. There are also plans to analyze the influence of trains crossing the viaduct in opposite directions, which has already been briefly discussed in [22].

3.2 Soil layers

The dynamic analysis, in principle, involves soils of infinite dimensions represented by a finite model. Therefore, special transmitting, absorbing or non-reflecting boundaries were introduced to the artificial model boundaries. A number of these were suggested in the past making use of various mathematical or physical principles, but all of them are mathematically equivalent, and must have comparable wave-absorbing attributes [25]. Unfortunately, none of the transmitting boundaries can fully prevent all possible reflections under the full range of possible incident angles. The better the performance of the absorbing boundary: the smaller the model that can be used. Lysmer's boundary according to [19] was checked and implemented in the FE model introducing the following viscous damping coefficient in normal, c_n, and tangential, c_t, directions:

$$c_n = \rho v_p, \; c_t = \rho v_s \tag{3}$$

where ρ is the soil density and v_p and v_s are velocities of propagation of pressure (primary) and shear (secondary) waves. These dampers absorb effectively pressure and shear waves, but not Rayleigh superficial waves. Nevertheless, in previous work

[20] Lysmer's damper performance was found satisfactory, even at the soil surface, if introduced at a reasonable distance from the source. Despite LS-DYNA capability of direct definition of non-reflecting boundaries, for better control and possible adaptation, it was decided to create the boundary "manually" on all lateral and bottom surfaces.

As referred to in Section 2, the miocene substrate can be characterized as an effectively stiff soil and was, therefore, chosen as an appropriate base for the foundations; 3m of this substrate were still considered, meaning that the structure is represented unpto22m below the soil surface. Only 6m of this active soil layer are included in the FE model. The "missing" layer of 16m depth, *i.e.* till the depth where rigid constraints are assumed, is substituted by representative springs [20] with the following stiffnesses in the normal and tangential directions, k_n and k_t, respectively:

$$k_n = \frac{\lambda + 2\mu}{H - h} = \frac{E(1-\nu)}{(1+\nu)(1-2\nu)(H-h)} = \frac{E^{oed}}{(H-h)} \tag{4}$$

$$k_t = \frac{\mu}{H - h} = \frac{E}{2(1+\nu)(H-h)} = \frac{G}{(H-h)} \tag{5}$$

where λ, μ, E, E^{oed}, G and ν are the two Lame´s constants, Young´s modulus, oedometer modulus, shear modulus and Poisson´s ratio of the replaced soil. H is the active depth and h is the depth of the soil in the model. As a result of the presence of different soil layers within $H - h$, equivalent springs were used.

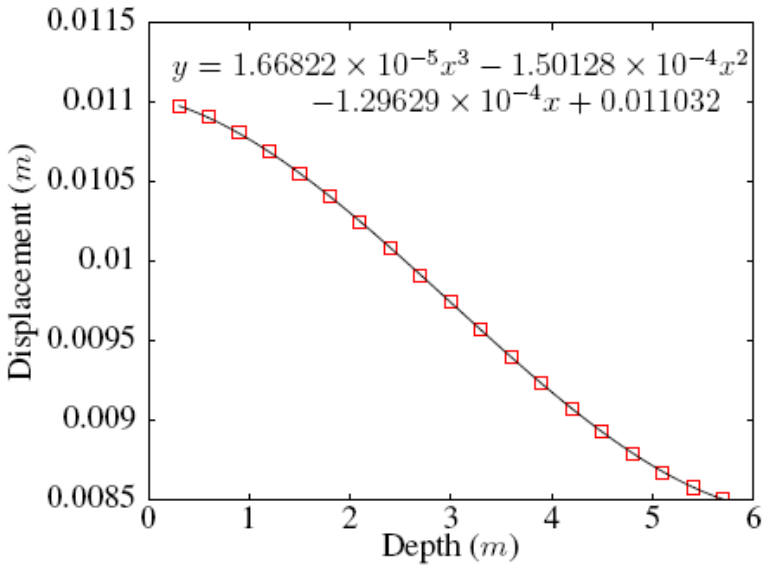

Figure 6: Cubic trend-line approximation of the displacement originated by uniform unit pressure with respect to depth

Regarding lateral springs, analysis that incorporates the effect of consolidation was accomplished. First of all, a cube of constrained soil subjected to its own weight was analysed and the displacement distribution caused by the uniform unit pressure was used as a base of springs stiffness variation with depth. Numerical values were approximated by the cubic trend-line represented in Figure 6. Then, the reference top displacement was established from fundamental equations of elasticity in the cylindrical coordinates, accounting, in this way, for geometric damping of a unit pressure applied to a vertical cylindrical surface.

Representative stiffnesses of lateral springs were certified by the natural frequencies calculation. First of all, it is worthwhile to remark, that it is a common practice to remove soil density in the natural frequencies calculation of a structure that is founded on soil. This way it is ensured that the soil provides the realistic flexibility of the foundation, and, at the same time, low frequencies that can be associated with spurious soil vibrations do not interfere with the vibration modes of the structure. In order to certify the values of the stiffnesses of the lateral springs, it was shown that the frequencies values are independent of the width of the surrounding soil considered.

Results are summarized in Table 2. First, ten natural frequencies were extracted from analyses that considered nine different values for the width of the surrounding soil measured from the pier central axis. To each of these cases, different values of the lateral springs were assigned. Generally speaking, the larger the soil: the softer the lateral spring. As can be seen, frequencies are practically independent from these choices, therefore the lowest value, 7m, was implemented in the model used for factorial analyses. All frequencies correspond to global vibration modes.

Mode shapes are exemplified in Figure 7. The first three bending modes (*i.e.* the bending of the deck on its transversal plan) are the 5th, the 7th and the 8th mode, respectively (Figure 7e), 7g), 7h)). A simple check shows that the value of 4.73Hz is comparable with the approximate value, obtained for a simply supported beam represented by the middle span. Using Figure 3, the sectional area and moment of inertia of the deck are $8.2m^2$ and $5.4m^4$, respectively, thus including the mass per length of 23.4ton/m, a bending frequency is 5.0Hz, which is close to the numerical

Width [m]	Natural Frequencies [Hz]									
7	2.60	3.47	3.75	4.53	4.73	4.92	5.44	6.44	7.72	9.21
10	2.57	3.38	3.73	4.50	4.73	4.84	5.44	6.44	7.70	9.19
13	2.56	3.35	3.71	4.48	4.73	4.82	5.44	6.44	7.69	9.19
15	2.55	3.34	3.71	4.48	4.73	4.81	5.44	6.44	7.69	9.19
17	2.55	3.33	3.71	4.48	4.73	4.81	5.44	6.44	7.69	9.19
20	2.55	3.33	3.71	4.48	4.73	4.82	5.44	6.44	7.69	9.19
23	2.55	3.33	3.71	4.48	4.73	4.82	5.44	6.44	7.69	9.19
25	2.55	3.33	3.71	4.48	4.73	4.82	5.44	6.44	7.69	9.19
27	2.55	3.33	3.71	4.48	4.73	4.82	5.44	6.44	7.69	9.19

Table 2: Natural frequencies for different values of the soil width and lateral springs

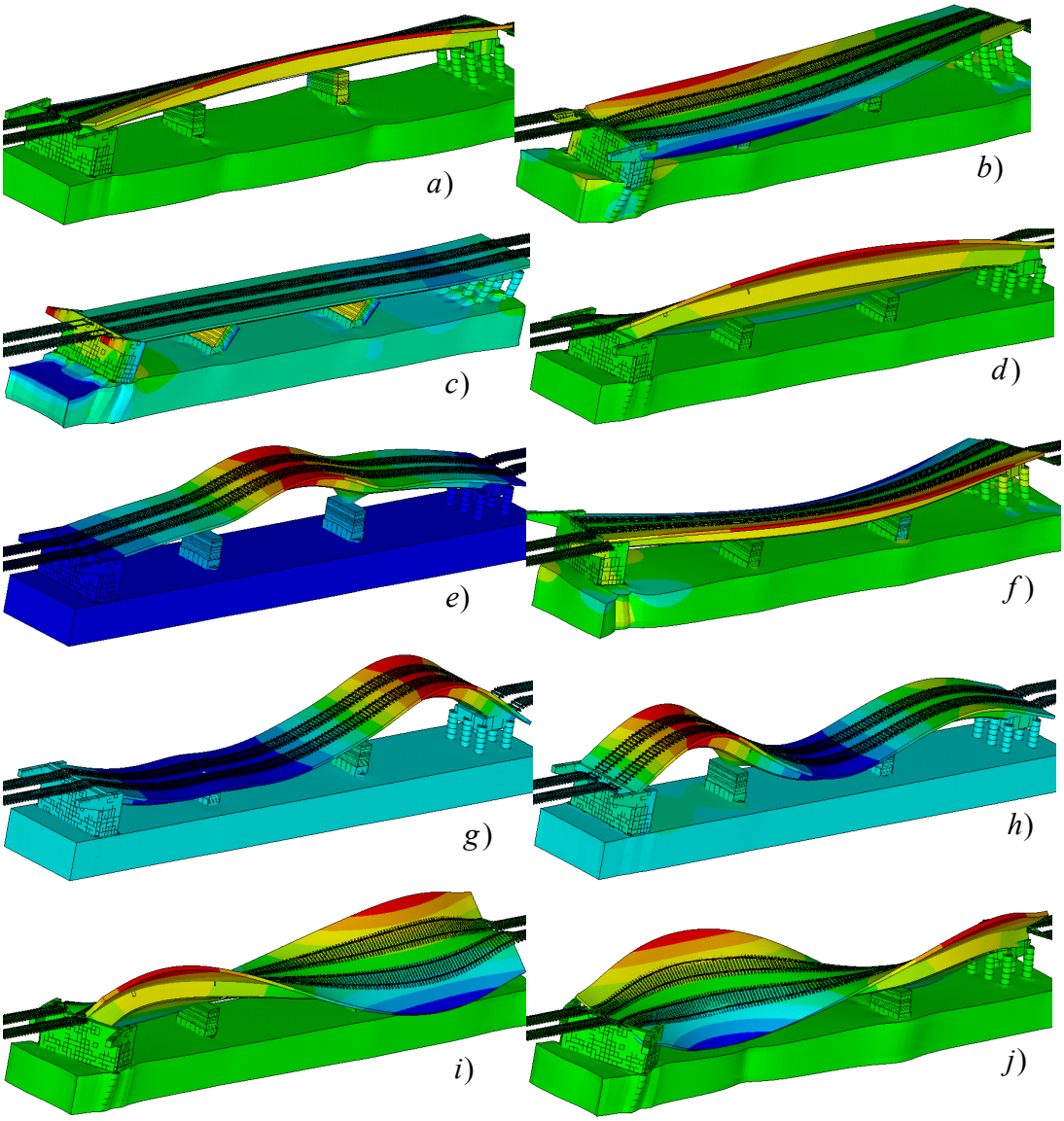

Figure 7: First ten vibration modes; contours correspond to normalized vertical displacement

value. The fundamental frequency corresponds to a lateral movement accompanied by the torsion of the deck around the longitudinal axis (Figure 7a), the third mode stands for the longitudinal movement accompanied by the bending of the piers on their own plan (Figure 7 c) and the last two modes represent torsional movements of the deck (Figure 7 i),7 j)).

In summary, the soil part included in the FE model for explicit dynamic analyses has 6m depth, 14m width and its density is obviously incorporated. Soil material damping of 7% is introduced according to [23].

3.3 Ballast and rail-pads

The finite element structure implemented is a three-dimensional extension of the system used in [24]. A scheme of the system is displayed in Figure 8.

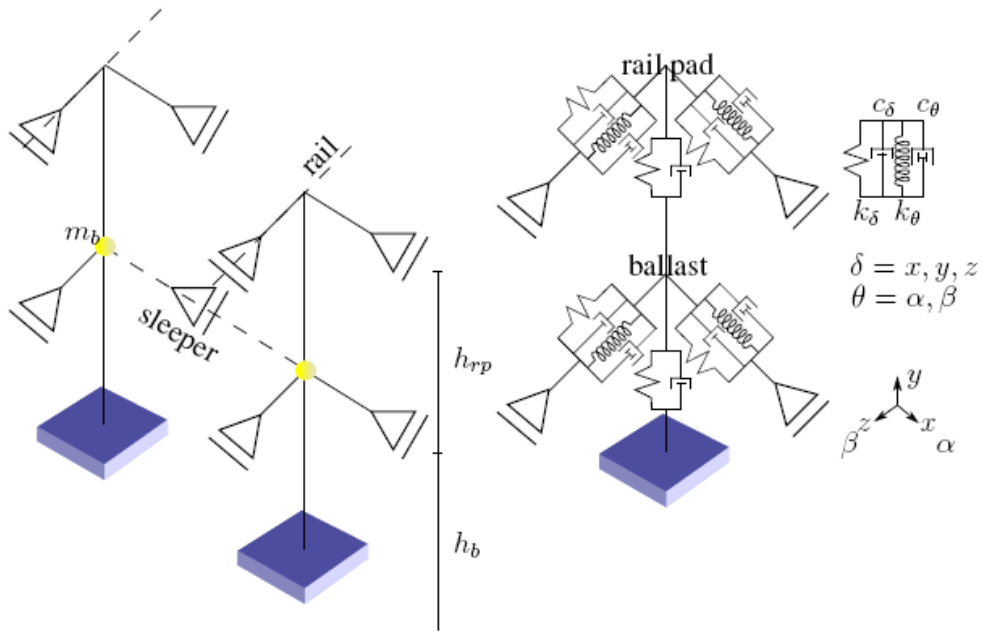

Figure 8: Three-dimensional spring/damper system

The ballast and rail-pads are idealized as a set of linear and rotational springs and dampers coupled together. The linear springs and dampers act in the three directions; rotational springs and dampers are introduced only in longitudinal and lateral directions. This representation is introduced separately for the ballast (two systems under each sleeper) and for each rail-pad. The ballast mass within the cone that contains the portion that is dynamically activated by the moving load under each sleeper is estimated according to [26], see Figure 9.

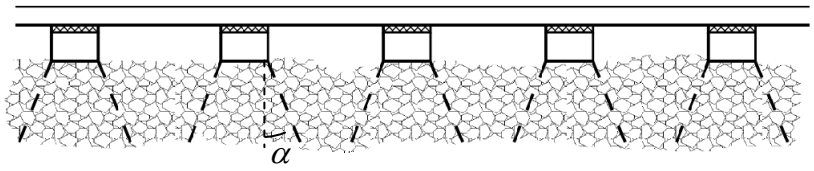

Figure 9: The ballast cone

This mass is inserted as a mass element, m_b, and placed directly on the sleeper. There are two mass elements, m_b, placed on each sleeper at the same position as the springs systems are connected to the sleeper (see Figure 8). The remaining ballast that acts only by its own weight on the deck was omitted because its influence is negligible. The angle of the ballast cone selected is $\alpha = 40°$, which is quite large,

thus caused by the ballast cones overlapping and their bases completely covering the deck surface. In this case, the neglected ballast mass is around 1.8ton/m. Distance between the systems described above in longitudinal direction is 0.6m. Material data are summarized in Table 3.

Parameter	Value	Parameter	Value
h_{rp}	0.196m	c_β - ballast	394kNs
h_b	0.30m	k_y – rail pad	280000kN/m
m_b	0.3225ton	c_y – rail pad	50kNs/m
k_y - ballast	120000kN/m	k_x – rail pad	50000kN/m
c_y - ballast	70kNs/m	c_x – rail pad	10kNs/m
k_x - ballast	40000kN/m	k_z – rail pad	50000kN/m
c_x - ballast	52kNs/m	c_z – rail pad	10kNs/m
k_z - ballast	40000kN/m	k_α - rail pad	597kNm
c_z - ballast	52kNs/m	c_α - rail pad	0.107kNs
k_α - ballast	676kNm	k_β - rail pad	597kNm
c_α - ballast	394kNs	c_β - rail pad	0.107kNs
k_β - ballast	676kNm		

Table 3: Material and geometrical data of the spring/damper system

3.4 Other materials

The viaduct is exclusively made from pre-stressed concrete, the deck and piles (C4555) being more resistant than the pillars and foundation block (C3037). PSC stands for pre-stressed concrete used in sleepers.

Material	E (GPa)	v	ρ (ton/m^3)
C3037	33	0.3	2.5
C4555	36	0.3	2.5
PSC	30	0.2	2.054

Table 4: Material data for concrete parts

Property	Beam (2 UIC60)
Young's modulus E (GPa)	210
Poisson's ratio v	0.3
Density ρ (kg/m^3)	7800
Cross-section area A (m^2)	$76.84 \cdot 10^{-4}$
Moment of inertia I (m^4)	$3055 \cdot 10^{-8}$

Table 5: UIC60 rail data

Concrete material data are summarized in Table 4, for UIC60 rail in Table 5. Regarding the concrete material, some analyses were run with no material damping,

others with material damping of 5%. Damping in steel rails was neglected. The finite element model is shown in Figure 10.

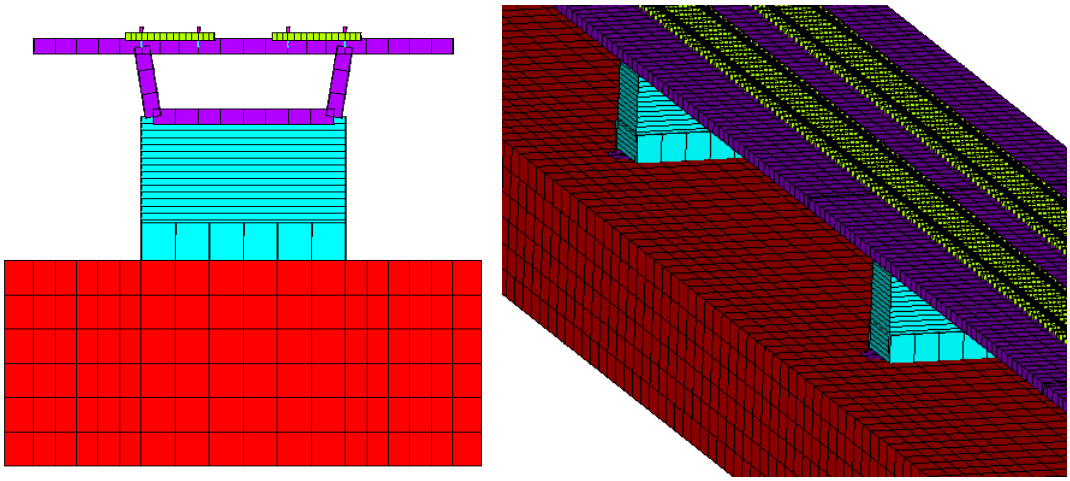

Figure 10: Frontal (left) and perspective (right) views

4 Results

Explicit analysis is performed in LS-DYNA software with a default time step calculated according to the element sizes and properties as 0.017ms, although the output was only written in 500 sets, *i.e.* each 5.88ms. Mesh size is variable over the model; it gradually increases from 10cm in rail to 1m in soil. It was verified numerically that soil elements are of sufficient size. Typical deflection curves of the external rail, the sleeper's level, and the deck along a line directly underneath the rail, is shown in Figure 11.

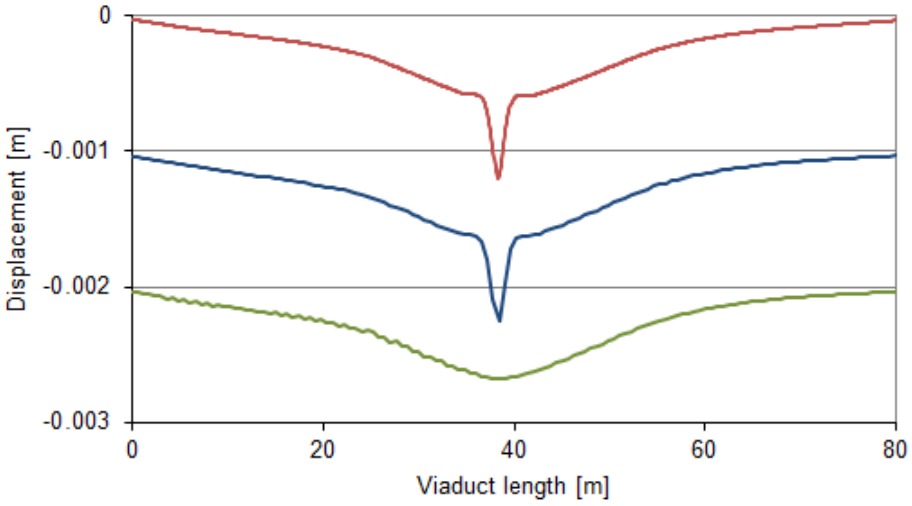

Figure 11: Deflection of the external rail (top curve), the sleeper (middle curve) and the deck (bottom curve)

For better clarity of the results, deflections in the sleepers and in the deck are plotted against a reference line at -0.001m and -0.002m, respectively. It is seen that the rail deflection is accentuated within a region of approximately 3m, which encompasses 5 sleepers. This deflection peak propagates into sleepers. A possible attenuation depends on whether the load is above the sleeper or between sleepers. Figure 11 shows the load position above the sleeper. More efficient attenuation is caused by the ballast layer, as expected. Deck deflection is, therefore, smooth.

Accelerations are shown in Figures 12-15. For better clarity of the results, accelerations in the sleepers and deck are plotted against a reference line at -80m/s2 and -120m/s2, respectively. In addition, accelerations in the sleepers and in the deck are scaled by a factor of 10 and 100, respectively. In this case, concrete damping of 5% was included.

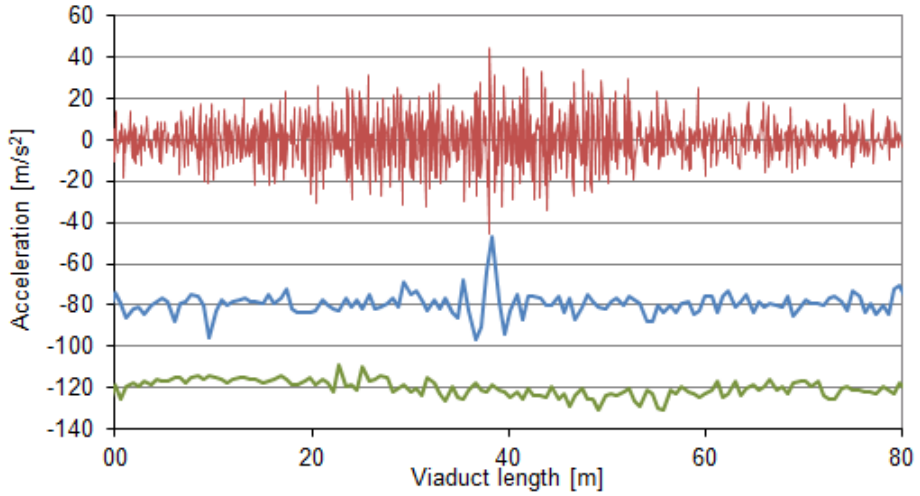

Figure 12: Accelerations of the external rail (top curve), the sleeper (middle curve) and the deck (bottom curve)

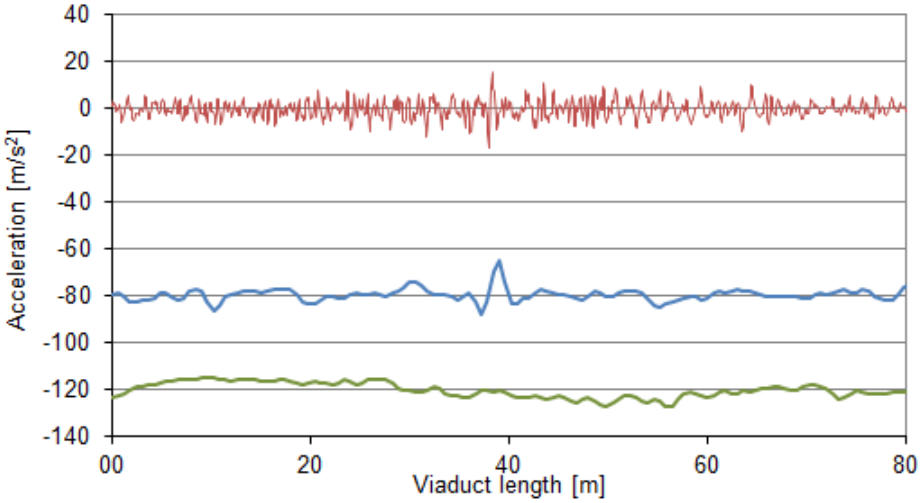

Figure 13: Accelerations of the external rail (top curve), the sleeper (middle curve) and the deck (bottom curve) filtered up to 30 Hz

When filters are applied, significant decrease is seen in rail accelerations while in sleepers and deck the original values already corresponded to relatively low frequencies. For a better understanding, in Figure 14, sleepers and deck accelerations are compared. Different curves correspond to original values, and values are filtered by 40 Hz and 30Hz, respectively. It is seen, that there are no big differences between the corresponding curves.

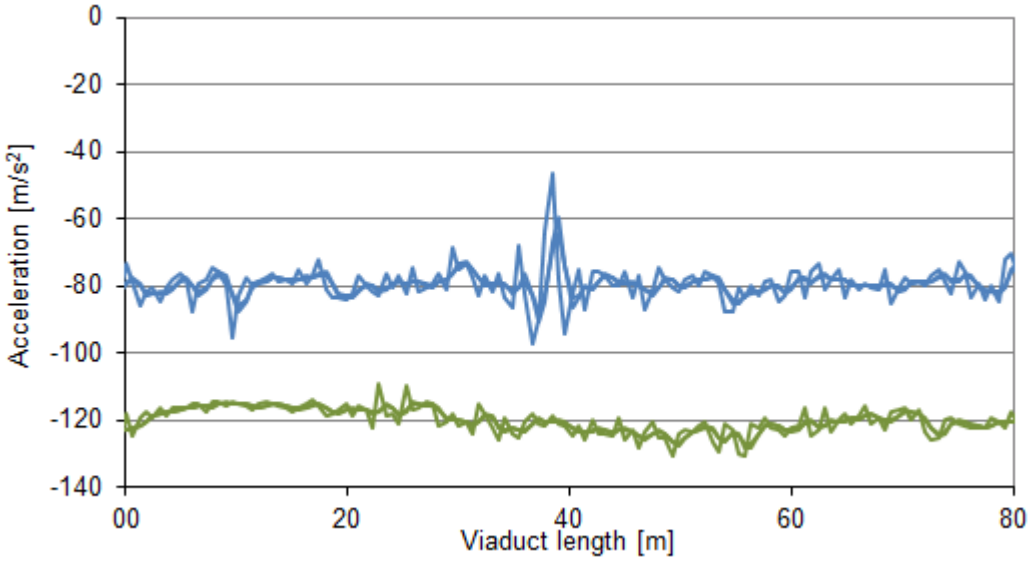

Figure 14: Accelerations in the sleepers (top curves) and the deck (bottom curves): overlaid curves correspond to original values and values filtered by 40Hz and 30Hz

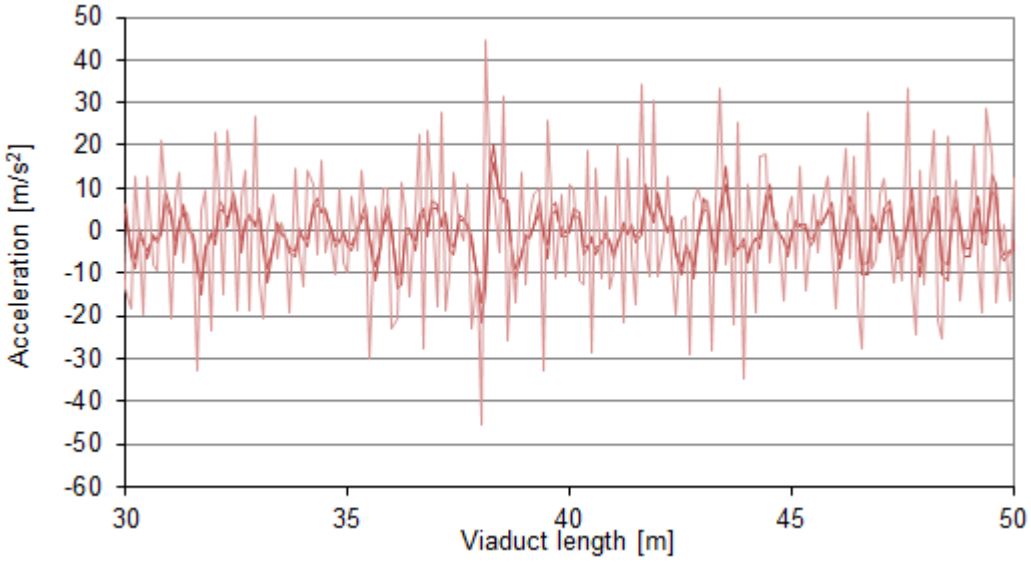

Figure 15: Accelerations in rails: light curve corresponds to original values and overlaid curves to values filtered by 40Hz and 30Hz

This is not true for rail accelerations, as exemplified in Figure 15. Frequency of excitation as a result of the moving force is naturally low if considered as excitation from passaging over simply supported beams of lengths equal to the viaduct spans (around 1Hz in our case). However, excitation frequency arising from load passage over sleepers is around 83 Hz. In the numerical treatment the time step is still small enough, therefore no filters were applied.

The statistics toolbox of Matlab software [27] was used to produce histograms of the key results, half normal plots with relevant factors and their interactions pointed out, and ANOVA tables. The analysis of the results is based on these three types of statistical output.

The selected factors, their variations and key results are presented in Table 6. The variations were introduced in a way that the average of the low and high factor value equated to the referenced value given in previous sections.

From the table it can be seen that all factors are qualitative. Two levels of full and fractional experimentations were analysed. Only some results will be presented. In Figure 16 half-normal probability plots of peak displacements and peak accelerations at the deck level (under the external rail) are shown and compared from the full and fractional factorial analysis.

There are 2^6=64 runs in the full factorial design. Fractional factorial design 2^{6-1}_{VI} analysis used 32 runs already performed. As a result of the high resolution no main effect or two-factor interaction are confounded with any other main effect or two-factor interaction. The experimentation was defined as the best half-fraction, *i.e.* in the way that the last effect F was confounded with the interaction of the first five effects, F=EDCBA. It is worthwhile to say that this does not mean that factor F was considered as less significant. The same results would be obtained for other choices.

Factors (variation)	Key results - Peak acceleration (vertical) - Peak displacement (vertical)
A. Ballast stiffness (40%)	rail level
B. Concrete stiffness (6%)	sleeper level
C. Soil stiffness (30%)	deck under external rail
D. Train speed (3%)	deck left extremity
E. Ballast damping (30%)	deck right extremity
F. Railpad damping (15%)	soil level (in line with pillars axes)

Table 6: Factors, their variation and key results

The following results are presented for the response evaluated with no material damping in the concrete since this assumption sharpened the differences under study. However, more realistic modelling of 5% concrete damping was also analysed. Small discrepancies were found in maximum displacements. Acceleration

peaks, especially at the concrete deck, were more or less ten times lower, but the main and combined effects remained the same.

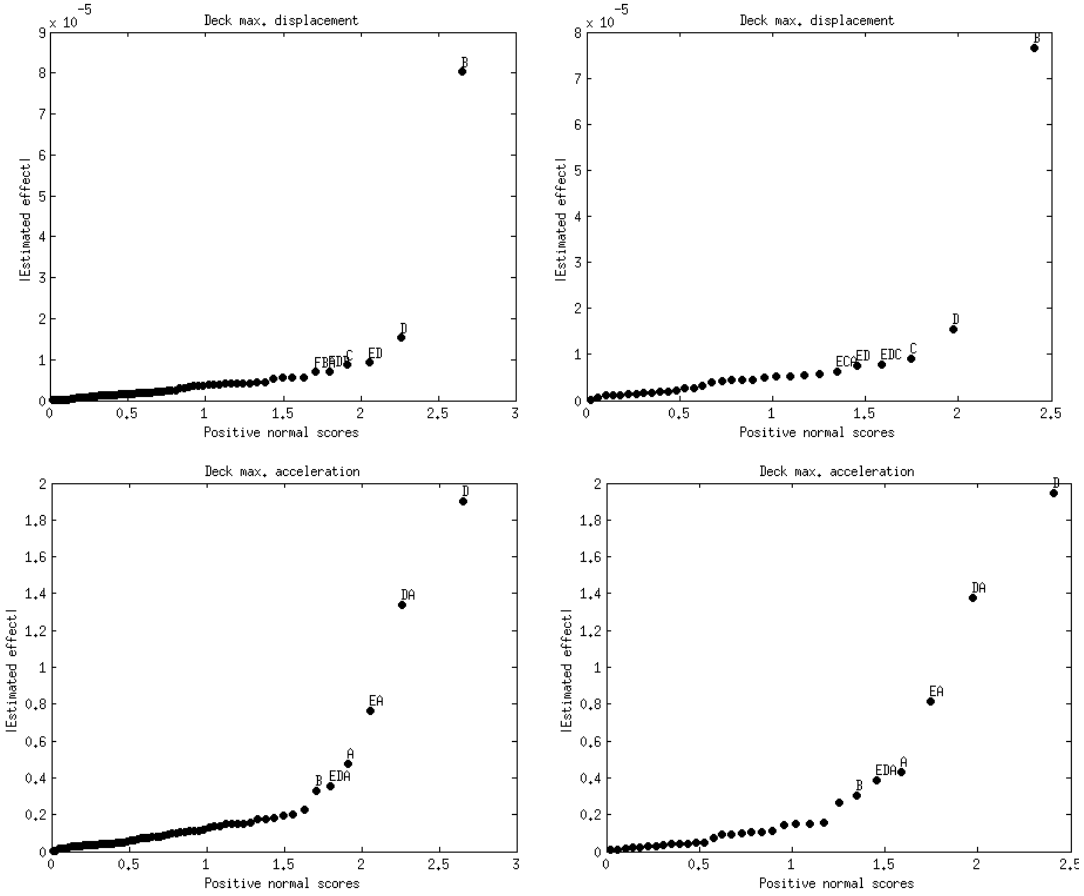

Figure 16: Half-normal probability plots of peak displacement and acceleration at the deck level under the external rail (left – full, right – fractional)

First of all, it is seen that results of full and fraction factorial experimentations are very similar, justifying the possibility of fractional factorial analysis implementation and significantly reducing the number of runs. From the graphs, it is seen that main and two-factor interaction responses from the full and fractional design are basically the same; some differences are noticeable for deck displacement. The other difference between the graphs is that the fractional design removes the noise that is not useful.

Next, it can be concluded that regarding the peak displacement the concrete stiffness is the leading factor. This means that this factor should be carefully controlled during design and construction. This also means that if measurements of displacements are planned for in-situ experiment, they should be accomplished on the deck. In this particular case, unfortunately, the deck surface under the rail is inaccessible for measurement. On the other hand, concrete stiffness could be the factor that may tune the FE model more easily.

Regarding the peak acceleration, the situation is completely different. Interactions are very strong and, therefore, it is impossible to take conclusions from the main effects, because the main effects should be individually interpreted only if there is no evidence that this variable interacts with the others.

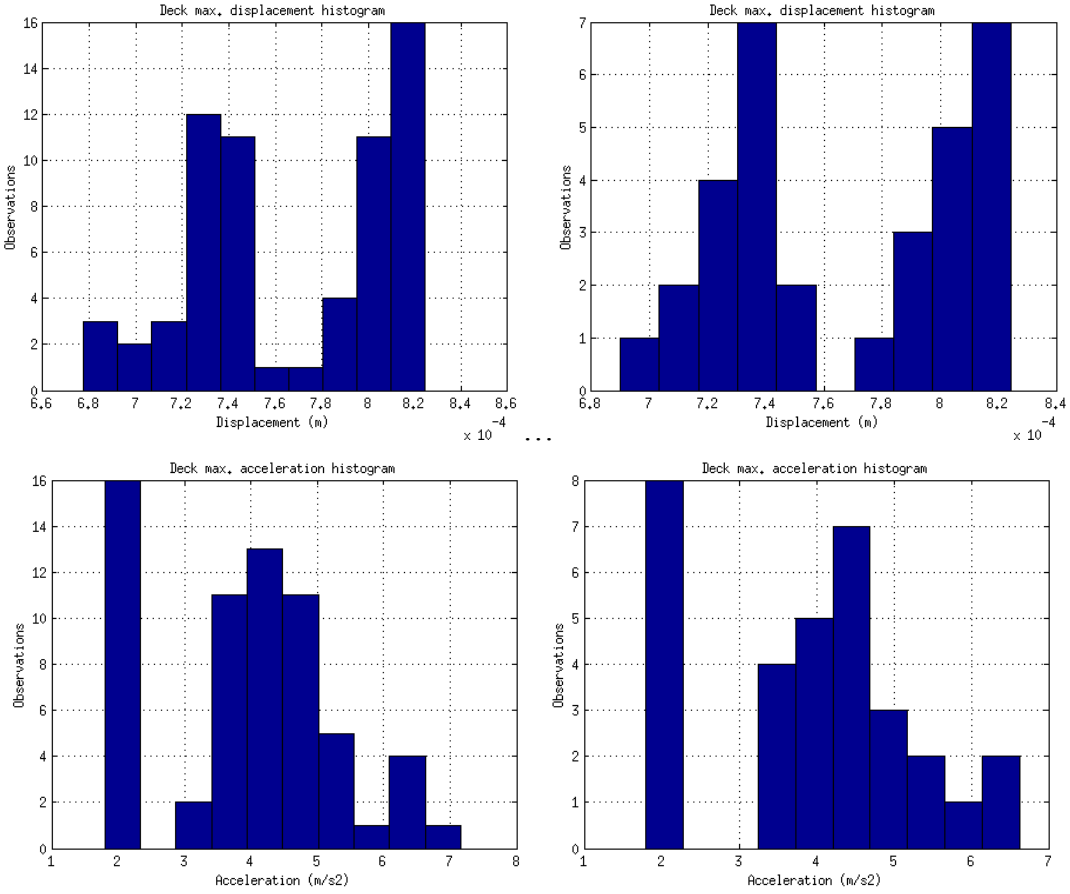

Figure 17: Results histograms of peak displacement and acceleration at the deck level under the external rail (left – full, right – fractional)

Further examination is required directed to interactions between ballast stiffness, damping and train velocity. On the other hand, the main effect of concrete stiffness does not play an important role. For the same reasons, in-situ measurement of peak accelerations at the deck level would not offer uniquely interpretable information for FE model calibration. It is worthwhile to point out the importance of ballast addition in the model. Usually, for the sake of simplicity, this part of the FE model is omitted, as in [17]. Results obtained here show that such omissions can cause a misinterpretation of the results, because, traditionally, accelerations are measured in in-situ tests.

The results presented in Figure 16, can also be viewed in the form of histograms and ANOVA tables. Histograms are presented in Figure 17. There are a significant number of combinations which lead to a substantial decrease in the peak

acceleration. It can be concluded that it would be worthwhile to analyze these combinations with the objective of mitigating the vibrations.

ANOVA tables are included in Appendix. Conclusions from ANOVA tables are basically the same as from half-normal plots.

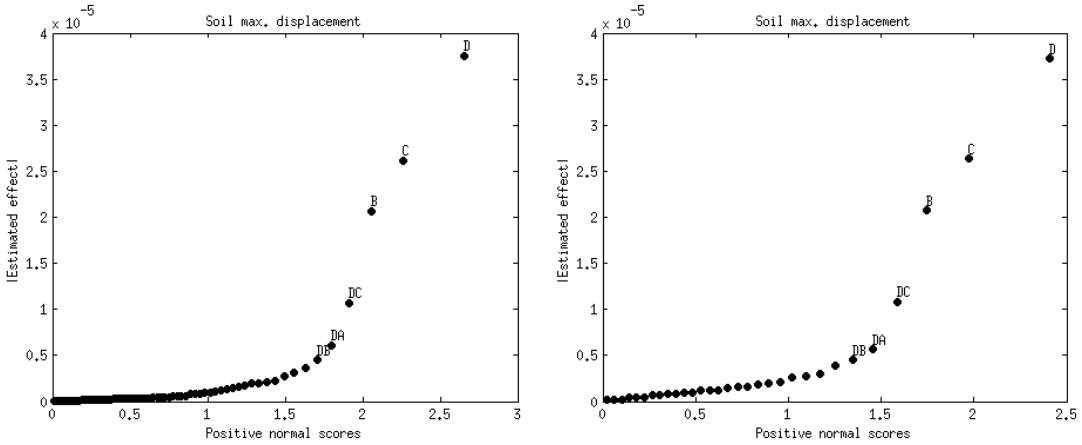

Figure 18: Half-normal probability plots of peak displacement on the soil level (left – full, right – fractional)

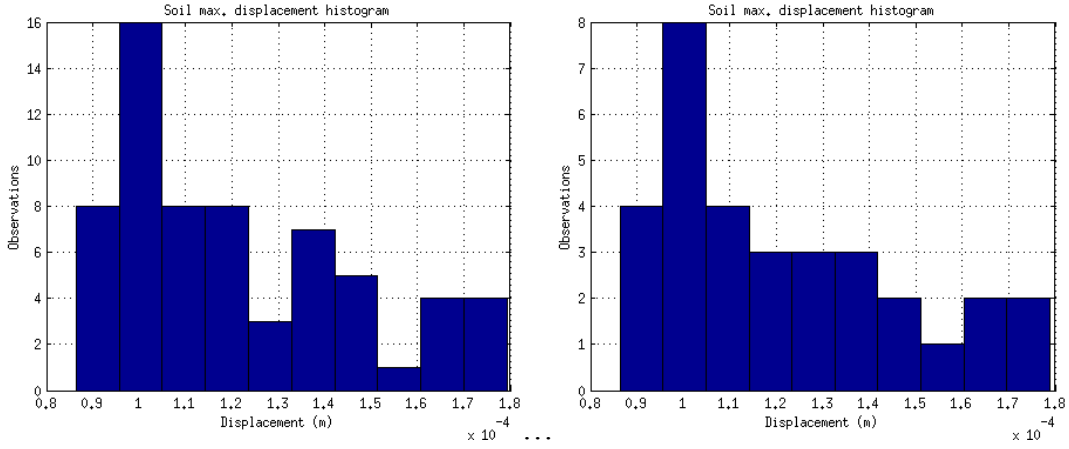

Figure 19: Results histograms of peak displacement on the soil level (left – full, right – fractional)

Regarding soil vibrations, maximum displacements were recorded on the soil level, in line with pillars middle axes, and in the vertical direction. From half-normal plots of full and fractional analyses (Figure 18) it is possible to conclude that main effects are dominant. It is, therefore, possible to draw several conclusions and establish that the dominant factors are the train speed, followed by the soil stiffness and, in third place, the concrete stiffness. Histograms are shown in Figure 19. Most combinations lead to a response decrease.

5 Conclusions

The qualitative influence of several model parameters on the dynamic response of a railways viaduct, modelled after an actual structure located in Santana do Cartaxo, Portugal, was analysed through a parametric statistical analysis. The statistical theory proved to be relevant, meaningful and easy to implement.

Two level factorial designs were used. It is known that they are not able to explore fully a wide region in the factor space, but they can indicate trends and directions for further exploration. Here, it was applied to peak displacements and peak accelerations. Peak displacements at the deck level showed the dominating influence of the concrete stiffness. This means that this factor should be carefully controlled during design and construction. This also means that if measurements of displacements are planned for in-situ experiment, they should be accomplished on the deck, and in addition, concrete stiffness can be the factor that may tune the FE model more easily. Peak displacements at the soil level showed the dominating influence of several main effects but no significant two-factor interactions. This means that traditional analysis by the variation of single factors can be implemented in analysis of soil vibrations induced by trains passing over the viaduct.

On the other hand, peak accelerations showed strong factor interactions. Hence, conclusions cannot be taken directly from two level factorial designs as further examination is necessary. It is worthwhile to point out the importance of ballast addition in the model. Usually, for the sake of simplicity this part of the FE model is omitted, but as it is shown here, such omissions can cause a misinterpretation of the results. There are a significant number of combinations leading to a substantial decrease in the peak acceleration. It can be concluded that it would be worthwhile to analyze these combination with the objective of mitigating the vibrations.

In summary, it has been shown how useful factorial screening can be, and how it can be implemented with regard to existing structures.

Acknowledgements

The authors greatly appreciate support from Fundação para a Ciência e a Tecnologia of the Portuguese Ministry of Science and Technology, supporting the execution of this work through the project grant PTDC/EME-PME/01419/2008: “SMARTRACK - SysteM dynamics Assessment of Railway TRACKs: a vehicle-infrastructure integrated approach”.

References

[1] C.E. Inglis, “A Mathematical Treatise on Vibration in Railway Bridges”, The Cambridge University Press, Cambridge, 1934.

[2] L. Frýba, “Dynamics of Railway Bridges”, Thomas Telford, London, Academia Prague, 1996.

[3] L. Frýba, “Vibration of Solids and Structures under Moving Loads”, Research Institute of Transport, Prague (1972), 3rd ed., Thomas Telford, London, 1999.

[4] B. Biondi, G. Muscolino, A. Sofi, "A substructure approach for the dynamic analysis of train-track-bridge system", Computers & Structures, 83(28–30), 2271–2281, 2005.
[5] M. Olsson, "Finite element, modal co-ordinate analysis of structures subjected to moving loads", Journal of Sound and Vibrations, 99(1), 1-12, 1985.
[6] M. Majka, M. Hartnett, "Effects of speed, load and damping on the dynamic response of railway bridges and vehicles", Computers & Structures, 86, 556-572, 2008.
[7] F. Cheli, R. Corradi, "On rail vehicle vibrations induced by track unevenness: Analysis of the excitation mechanism", Journal of Sound and Vibrations, 330, 3744-3765, 2011.
[8] C.P. Tan, S. Shore, "Response of horizontally curve bridge to moving load", Journal of the Structural Division: Proceedings of the ASCE, 94(9), 2135-2151, 1968.
[9] Y.B. Yang, J.D. Yau, Y.S. Wu, "Vehicle–Bridge Interaction Dynamics: With Applications to High-Speed Railways", World Scientific, 2004.
[10] R. Willis, "Preliminary Essay to the Appendix B: Experiments for Determining the Effects Produced by Causing Weights to Travel over Bars with Different Velocities", In G. Grey, *et al.*, "Report of the Commissioners Appointed to Inquire into the Application of Iron to Railway Structures", W. Clowes and Sons, London, 1849.
[11] G.G. Stokes, "Discussion of a differencial equation relating to the breaking of railway bridges", Transactions of the Cambridge Philosophical Society, 8, Part 5, 707-735, 1849.
[12] H. Zimmermann, "Die Schwingungen eines tragers mit bewegter last", Centralblatt der Bauverwaltung, 16(23), 249-251; (23A), 257-260; (24), 264-266; (26), 288, 1896. (in German)
[13] A.N. Krylov, (A.N. Kriloff), "Über die erzwungenen schwingungen von gleichformigen elastichen stäben", Mathematische Annalen, 61, 211-234, 1905. (in German)
[14] S.P. Timoshenko, "Forced vibration of prismatic bars", Izvestiya Kievskogo politekhnicheskogo institute, 1908. (in Russian); "Erzwungene schwingungen prismatischer stabe", Zeitschrift für Mathematik und Physik, 59(2), 163–203, 1911. (in German).
[15] A.N. Lowan, "On transverse oscillations of beams under the action of moving variable loads", Philosophical Magazine, Series 7, 19(127), 708–715, 1935.
[16] N.G. Bondar, "Dynamic calculation of beams subjected to a moving load", Issledovaniya po teorii sooruzhenii, Stroiizdat, Moscow, 6, 11-23, 1954. (in Russian)
[17] J. Wiberg, R. Karoumi, C. Pacoste, "Statistical screening of individual and joint effect of several modelling factors on the dynamic finite element response of a railway bridge", Computers & Structures, 2012. (online)
[18] G.E.P. Box, W.G. Hunter, J.S. Hunter, "Statistics for Experimenters: An Introduction to Design, Data Analysis, and Model Building", John Wiley and Sons, 1978.
[19] ANSYS, Inc., "Documentation for Release 12.1", Swanson Analysis Systems

IP, Inc., November 2009.
[20] J. Lysmer, R.L. Kuhlemeyer, "Finite dynamic model for infinite media", Journal of the Engineering Mechanics Division, ASCE, 95(EM4), 859-877, 1969.
[21] Z. Dimitrovová, A.F.S. Rodrigues, "An Enhanced Moving Window Method: Applications to High-Speed Tracks", in B.H.V. Topping, Y. Tsompanakis, (Editors), "Proceedings of the Thirteenth International Conference on Civil, Structural and Environmental Engineering Computing", Civil-Comp Press, Stirlingshire, UK, Paper 6, 2011. doi:10.4203/ccp.96.6
[22] A.H. Jesus, Z. Dimitrovová, M.A.G. Silva, "Dynamic Analysis of the Santana do Cartaxo Viaduct: Definition of the Experimental Verification using Statistical Analysis of the Numerical Results", in J. Pombo, (Editor), "Proceedings of the First International Conference on Railway Technology: Research, Development and Maintenance", Civil-Comp Press, Stirlingshire, UK, Paper 5, 2012. doi:10.4203/ccp.98.5
[23] REFER EP, "Projecto de modernização da linha do norte sub-troço 1.4: Azambuja(excl.) - Vale de Santarém(Incl.), Projecto de execução, Volume 10 - Viaduto Santana do Cartaxo, Memória Descritiva e Justificativa – Geologia e Geotecnia, Memória Descritiva e Justificativa – Obra de Arte Revisão 1", Viaponte, September 2003. (in Portuguese)
[24] T. Mazilu, M. Dumitriu, "On the Steady State Interaction between an Asymmetric Wheelset and Track", in B.H.V. Topping, Y. Tsompanakis, (Editors), "Proceedings of the Thirteenth International Conference on Civil, Structural and Environmental Engineering Computing", Civil-Comp Press, Stirlingshire, UK, Paper 27, 2011. doi:10.4203/ccp.96.27
[25] E. Kausel, "Local transmitting boundaries", Journal of Engineering Mechanics, 114, 1011-1027, 1988.
[26] W.M. Zhaia, K.Y. Wanga, J.H. Lin, "Modelling and experiment of railway ballast vibrations", Journal of Sound and Vibration, 270, 673–683, 2004.
[27] "Release R2009a Documentation for MATLAB", The MathWorks, Inc., 2009.

Appendix

Source	SumSq.	d.f.	MeanSq.	F	Prob>F
B	1,03E-01	1	1,03E-01	832.22	1,08E-29
D	3,75E-03	1	3,75E-03	30.34	9,05E-01
D*E	1,38E-03	1	1,38E-03	11.18	1,47E+03
C	1,24E-03	1	1,24E-03	9.99	2,52E+03
B*D*F	8,12E-04	1	8,12E-04	6.56	1,31E+04
A*B*F	7,91E-04	1	7,91E-04	6.39	1,42E+04
Error	7,05E-03	57	1,24E-04		
Total	1,18E-01	63			

Table A: ANOVA table for peak displacement at the deck level under the external rail – full factorial analysis

Source	SumSq.	d.f.	MeanSq.	F	Prob>F
B	4,70E-02	1	4,70E-02	510.21	3,77E-12
D	1,89E-03	1	1,89E-03	20.53	1,26E+02
C	6,48E-04	1	6,48E-04	7.03	1,37E+04
C*D*E	4,95E-04	1	4,95E-04	5.37	2,89E+04
D*E	4,66E-04	1	4,66E-04	5.05	3,36E+04
A*C*E	3,19E-04	1	3,19E-04	3.47	7,44E+04
Error	2,30E-03	25	9,21E-05		
Total	5,31E-02	31			

Table B: ANOVA table for peak displacement at the deck level under the external rail – fractional factorial analysis

Source	SumSq.	d.f.	MeanSq.	F	Prob>F
D	5,80E+07	1	5,80E+07	357.69	3,09E-20
A*D	2,87E+07	1	2,87E+07	177.18	3,90E-13
A*E	9,40E+06	1	9,40E+06	57.98	3,01E-04
A	3,59E+06	1	3,59E+06	22.11	1,68E+01
A*D*E	2,05E+06	1	2,05E+06	12.62	7,73E+02
B	1,75E+06	1	1,75E+06	10.81	1,74E+03
Error	9,24E+06	57	1,62E+05		
Total	1,13E+08	63			

Table C: ANOVA table for peak acceleration at the deck level under the external rail – full factorial analysis

Source	SumSq.	d.f.	MeanSq.	F	Prob>F
D	3,03E+07	1	3,03E+07	395.63	7,70E-11
A*D	1,52E+07	1	1,52E+07	197.95	2,21E-07
A*E	5,29E+06	1	5,29E+06	69.00	1,18E-02
A	1,50E+06	1	1,50E+06	19.60	1,65E+02
A*D*E	1,20E+06	1	1,20E+06	15.64	5,57E+02
B	7,37E+05	1	7,37E+05	9.61	4,74E+03
Error	1,92E+06	25	7,67E+04		
Total	5,62E+07	31			

Table D: ANOVA table for peak acceleration at the deck level under the external rail – fractional factorial analysis